Predictive value of LN metastasis detected by 18F-FDG PET/CT in patients with papillary thyroid cancer receiving iodine-131 radiotherapy

CHAO LI[1*], JIAN ZHANG[2*] and HUI WANG[1]

[1]Department of Nuclear Medicine, Xinhua Hospital, Shanghai Jiao Tong University School of Medicine, Shanghai 200092; [2]Universal Medical Imaging Diagnostic Center, Shanghai 201103, P.R. China

Abstract. The aim of the present study was to predict the prognostic value of 18F-fluorodeoxyglucose (FDG) positron emission tomography/computed tomography (PET/CT) in the metastatic lymph nodes (mLNs) of patients with papillary thyroid carcinoma (PTC) with a negative iodine-131 (^{131}I) whole-body scan (WBS). The present retrospective study included 32 patients with PTC undergoing standard surgery and radioiodine treatment. All patients received 18F-FDG PET/CT imaging prior to and following therapy. All mLNs were divided into an effective treatment group (group A) and ineffective treatment group (group B) based on the PET Response Criteria in Solid Tumors 1.0 guidelines. All the patients were followed up for ≥9 months. A significant difference was identified in the peak standardized uptake value (SULpeak) between group B (7.85±3.20) and group A (5.36±2.19). A cut-off value of 5.85 was used to distinguish ineffective treatment of lesions from mLNs receiving radioactive ablation based on receiver operating characteristic (ROC) curve analysis with an area under the ROC curve of 0.755. Patients with a high SULpeak (P=0.003) and extrathyroidal extension (P=0.030), confirmed by pathology, more frequently exhibited a poor prognosis. In conclusion, tracer uptake of 18F-FDG for cervical metastatic nodes was revealed as a predictor for the clinical outcome of patients with PTC treated with radioiodine therapy. The present results also indicated that high SULpeak and extrathyroidal extension are poor predictors for patients with mLNs receiving ^{131}I therapy.

Introduction

Papillary thyroid carcinoma (PTC) is the most common type of thyroid tumor and despite developments in imaging techniques, the incidence rate of PTC has increased over the last decade (1). Locoregional lymph node (LN) metastasis is typically one of the first steps in the progression of PTC to distant metastasis from the thyroid (2,3). According to a previous report from the National Comprehensive Cancer Network, the LN metastasis rate in PTC is 50-80% (4).

The most effective therapeutic strategies for well-differentiated thyroid carcinoma are thyroid surgery and iodine-131 (^{131}I) radiotherapy (5). ^{131}I radiotherapy is not only appropriate for primary tumors but also for LN and distant metastasis (6). Kim *et al* (7) reported that for lesions with high serum thyroglobulin (Tg), a negative cervical sonography and an 18F-fluorodeoxyglucose (FDG) positron emission tomography (PET) scan exhibit limited therapeutic effect with ^{131}I therapy. Positron emission tomography and computed tomography (PET/CT) has been applied for the evaluation and monitoring of PTC and nodal metastasis, particularly for patients with elevated serum Tg levels but produced negative findings with an iodine-131 (^{131}I) whole-body scan (WBS) (8). Previously, small LNs have been detected with PET/CT, which are easily misdiagnosed by ^{131}I-WBS due to a low resolution and the presence of remnant thyroid tissue (9). To the best of our knowledge, the association between metastatic LNs (mLNs) and the effect of ^{131}I therapy has not yet been reported. The aim of the present retrospective study was to evaluate the clinical efficiency of 18F-FDG PET/CT in predicting the therapeutic response of mLNs in patients with PTC following ^{131}I therapy.

Patients and methods

Patients. The present retrospective study was approved by Ethics Committee of Xinhua Hospital Affiliated to Shanghai

Correspondence to: Professor Hui Wang, Department of Nuclear Medicine, Xinhua Hospital, Shanghai Jiao Tong University School of Medicine, 1665 Kongjiang Road, Shanghai 200092, P.R. China
E-mail: wanghui@xinhuamed.com.cn

[*]Contributed equally

Jiaotong University School of Medicine and the requirement for informed consent was waived. Between January 2012 and August 2017, 106 patients at the Nuclear Medicine Department of Xinhua Hospital Affiliated with The Shanghai Jiaotong University School of Medicine (Shanghai, China) were assessed based on the following criteria: i) All patients underwent a near-total or a total thyroidectomy; ii) patients received a PET/CT examination prior to their first and following their second or later ^{131}I radioiodine ablation treatment; iii) patients with LN metastasis were identified by fine-needle aspiration biopsy (FNAB), postoperative pathology and other clinical methods, including neck ultrasonography, CT, ^{131}I-WBS, and serum Tg and thyroglobulin-antibody levels. Patients were excluded if they had a history or coexistence of other metastasis, including lung or bone metastasis. In addition, patients were excluded if the LNs were not confirmed by pathology, biopsy or other clinical findings. In total, 74 patients were excluded, including 16 patients with bone metastasis, 35 patients with lung metastasis and 23 patients who did not possess appropriate evidence of LN metastasis. Therefore, 18 female and 14 male patients were enrolled in the present study.

mLNs. The mLNs involved in the present study were included according to the following criteria: i) The mLN was diagnosed by postoperative pathology or FNAB; ii) the LN had a positive ^{131}I accumulation on the ^{131}I WBS; iii) ultrasonographic features of malignant thyroid nodules included hypoechoic lesions, a longitudinal/transverse ratio <2, a blurred or spicular margin, microlobular contour, single or multiple microcalcifications, both internal and peripheral flow, and extrathyroidal extension or an interrupted and discontinuous echogenicity of a capsule (10); iv) a mLN on CT manifestations exhibited an unenhanced center and rim enhancement, with or without fine sand calcification and mottle calcification, or a LN with a spherical shape and minimal axial diameter (MAD) >10 mm (11) and an increase in size on follow-up CT; and v) a LN of spherical shape, peak standardized uptake value (SULpeak) >2.5 with a history of stimulated Tg level >10 ng/ml during thyroid hormone withdrawal. A total of 50 nodes were identified as mLNs.

18F-FDG PET/CT. PET/CT imaging was performed using a Biograph 64 PET/CT scanner (Siemens AG, Munich, Germany). Prior to 18F-FDG PET/CT, all patients were instructed not to eat for ≥6 h to maintain their serum glucose levels at <11.1 mmol/l prior to injection. Image acquisition started ~1 h (mean, 56±2 min; range, 50-60 min) following intravenous injection of FDG (3.7 megabecquerel/kg). The lowest possible milliampere setting on the scanner was used to acquire the CT scans for attenuation correction. The whole-body CT imaging was performed from the skull to the upper part of the thigh with 120 kV, 0.5 sec rotation, 3 mm slice thickness and 0.8 mm intervals. The PET scans were obtained immediately following the whole-body CT scan, including 5-7 bed positions (1.5 min acquisition time per bed position) over the same range as the CT scan. Prior to PET/CT imaging, the serum thyrotropin (TSH) levels of patients were maintained at 30 mU/l.

[131]I therapy and post-therapy ^{131}I whole-body scintigraphic imaging. Following radioiodine ablation of the residual normal thyroid tissue, 19 patients received a second dose of therapy and five also received an additional third dose of therapy. The TSH level was measured prior to ^{131}I administration and a minimum TSH of 30 mU/l was required. ^{131}I-NaI was orally administered, with activities ranging between 3.7 and 7.4 gigabecquerel (100-200 mCi). The ^{131}I WBS was conducted 3-4 days following ^{131}I administration, using a dual-head large-field γ camera with high energy collimators. An additional single-photon emission CT/CT (SPECT/CT) scan was performed with extensive cervical iodine accumulation on the WBS scan in four patients (4/32).

Imaging analysis. The acquired images were analyzed with Siemens True D (Syngo TrueD VE13A). The tracer uptake was expressed as a standardized uptake value, which was calculated according to the following formula: Measured activity concentration (Bq/ml) x body weight (g)/injected activity (Bq). To achieve a larger region of interest, the SULpeak that corrected for lean body mass was selected instead of the widely used single-pixel maximum standardized uptake value. The maximum standardized uptake has also been demonstrated to be subjected to upward bias in low-count studies compared with the SULpeak (12). All 18F-FDG PET/CT images and ^{131}I-WBS images were visually interpreted by two experienced nuclear physicians, and a final consensus was reached for all patients.

Statistical analysis. All quantitative data are expressed as the mean ± standard deviation. A χ^2 test and t-test were used to compare the SULpeak, minimum diameter, maximum diameter, LN zone, shape and density, punctate calcification, and the longitudinal and transverse ratios of the mLNs in the effective treatment group and ineffective treatment group. To assess the predictive role of SULpeak for the therapeutic effect, receiver operating characteristic (ROC) analysis was performed in both the effective treatment group and ineffective treatment group. The cut-off value was selected as 5.85, above which the best compromise between sensitivity and specificity could be achieved. Multivariate analysis of categorical variables was conducted using the survival analysis model. All statistical analysis was performed using SPSS software (version 17.0; SPSS, Inc., Chicago, IL, USA). P<0.05 was considered to indicate a statistically significant difference.

Results

Patients. Among the 32 enrolled patients, the mean ± standard deviation age was 40.6±10.6 years (range, 24-58 years). According to the 7th Edition of The TNM staging system from The American Joint Committee on Cancer (13), 18 patients had stage I disease, 6 patients had stage II disease, 3 patients had stage III disease and 5 patients had stage IV disease. During surgery, 13 patients were identified to have extrathyroidal extension and 18 patients had residual thyroid tissue on the initial ^{131}I WBS. In the present study, clinical serum outcomes of Tg were obtained under a TSH stimulated state <1 week prior to or following the PET/CT examination. Follow-up was performed ≥9 months following examination, with a mean follow-up time of 17.87±6.80 months (range, 9-36 months).

Table I. Characteristics of metastatic lymph nodes.

Characteristics	Mean (standard deviation), range	n (50)
Minimum axial diameter, mm	7.29 (2.42), 3.00-14.00	
Maximum axial diameter, mm	9.77 (2.66), 4.70-16.00	
Peak standardized uptake value	6.80 (3.06), 2.60-16.60	
Lymph node zone (41)		
I		0
II		14
III		9
IV		9
V		2
VI		15
VII		1
Spherical shape with solid density		34
Spherical shape with soft density		16
Longitudinal and transverse ratio (<2)		
Yes		38
No		12
Punctate calcification		
Yes		19
No		31

mLNs. A total of 50 lesions were diagnosed as mLNs in 32 patients, with 1-4 lesions identified per patient. A total of ten lesions were diagnosed by histopathological findings; eight were diagnosed by positive ^{131}I accumulation on the ^{131}I-WBS; ten were diagnosed by neck ultrasonography and ^{18}F-FDG PET with six lesions exhibiting a blurred margin, multiple microcalcifications, internal flow and peripheral flow, and four lesions exhibiting single microcalcification and extrathyroidal extension; and twelve lesions were diagnosed by CT and ^{18}F-FDG PET with seven lesions exhibiting a MAD >10 mm, and four lesions demonstrating an increase in size following ≥9 months. The characteristics of the mLNs are presented in Table I.

The metabolic response was determined separately for changes in the SULpeak based on the PET Response Criteria in Solid Tumors 1.0 (14). A complete response (CR) was defined as a complete resolution of abnormal ^{18}F-FDG uptake within measurable target lesions, such that the uptake was equal to or less than the mean healthy-liver activity on the follow-up examination. A partial response (PR) was defined as a decrease of >30% in any baseline PET parameter. Progressive disease (PD) was defined as an increase in any baseline PET parameter by >30% between the baseline and follow-up, or by the appearance of a new ^{18}F-FDG-avid lesion. Stable disease (SD) was defined as non-PD, non-PR and non-CR. All mLNs were divided into the following two groups: An effective treatment group (group A) and an ineffective treatment group (group B). The lesions in group A achieved either CR or PR, while the lesions in the group B achieved either SD or PD.

The standard uptake value of lean body mass (SUL) of the 29 mLNs in group B (mean, 7.85±3.20; range, 3.00-16.60)
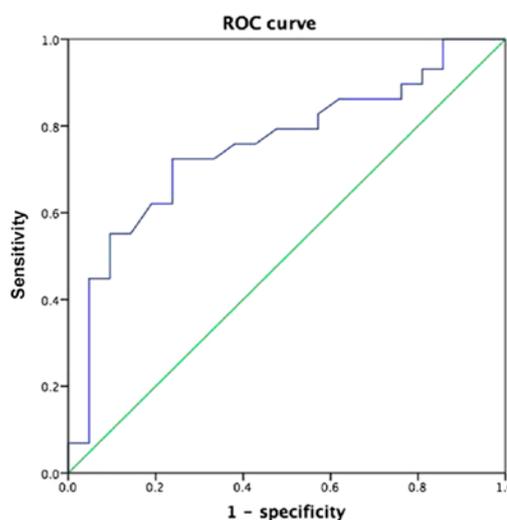

Figure 1. ROC curve of peak standardized uptake value to predict the therapeutic effect of lymph node metastasis (n=42). ROC, receiver operating characteristic.

was significantly higher compared with that of the 21 mLNs in group A (mean, 5.36±2.19; range, 2.60-12.80; P=0.027). A cut-off value of 5.85 was used to distinguish the ineffective treatment lesions from the mLNs receiving radioactive ablation based on the ROC curve analysis, with an area under the ROC curve (AUC) of 0.755. The accuracy of predicting the therapeutic effect of group A and group B was 76.19 and 72.4%, respectively (Fig. 1). Furthermore, a significant difference was identified in the shape and density between the two groups (P=0.044; Table II). However, the minimum diameter,

Table II. Clinical characteristics of metastatic lymph nodes in group A and group B prior to therapy.

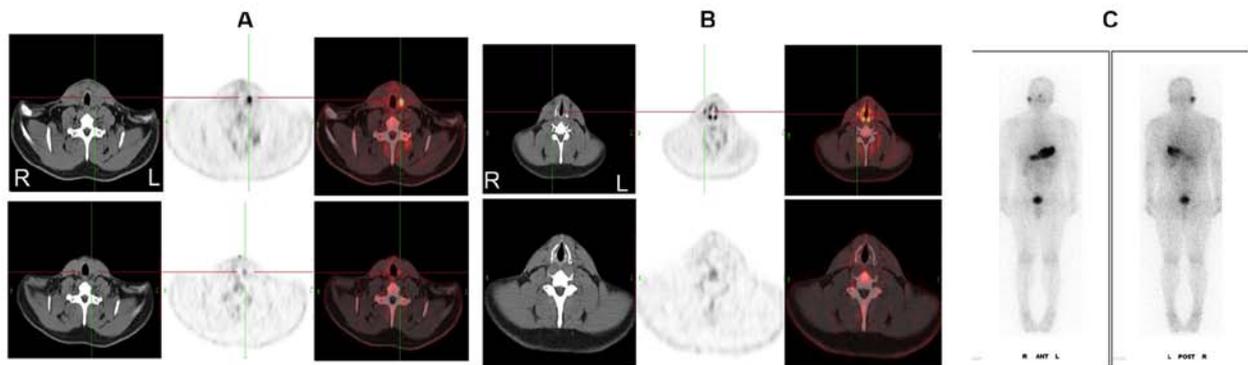| Characteristics	Group A	Group B	P-value
Number	21	29	0.422
Minimum diameter, mm			0.338
Mean (SD)	7.02 (2.16)	7.48 (2.61)	
Range	4.00-12.00	3.00-14.00	
Maximum diameter, mm			0.457
Mean (SD)	9.67 (2.40)	9.84 (2.86)	
Range	4.70-14.00	5.00-16.00	
Peak standardized uptake value			0.027
Mean (SD)	5.36 (2.19)	7.85 (3.20)	
Range	2.60-12.80	3.00-16.6	
Lymph node zone, n (41)			0.416
VI	5	10	
Non-VI	16	19	
Shape and density, n			0.044
Spherical shape with solid density	10	19	
Spherical shape with soft density	8	5	
Punctate calcification, n			0.242
Yes	6	13	
No	15	16	
Longitudinal and transverse ratios (<2), n			0.314
Yes	14	23	
No	7	6	

SD, standard deviation.

Figure 2. A 24-year-old male patient with papillary thyroid carcinoma with mLNs. The LNs detected by CT exhibited a spherical shape and a homogeneous density, which revealed hypermetabolic LNs in the (A) left side of the neck and in the (B) right side of the neck. The standardized uptake values of the LNs on the PET/CT images before (upper images) and after (lower images) [131]I therapy were 5.7, 3.5, and 3.0, 1.1, respectively. (C) [131]I whole-body scan image revealed no ^{131}I accumulation in the two mLNs. The lesions achieved a partial response (LN in the left neck) and complete response (LN in the right neck), respectively. mLN, metastatic lymph node; LN, lymph node; PET, positron emission tomography; CT, computed tomography; ^{131}I, iodine-131.

maximum diameter, LN zone, punctate calcification, and longitudinal and transverse ratios (<2) demonstrated no significant difference between the two groups (P>0.05; Table II).

The effective treatment of mLNs following ^{131}I radiotherapy was independently associated with SULpeak and extrathyroidal extension. The sex, stage, size and location of LN, Tg level, spherical shape with solid density, LN zone, punctate calcification, longitudinal and transverse ratios (<2), and residual thyriod tissue prior to therapy were not identified as risk factors for ^{131}I therapy (Table III).

In this study, seven mLNs were found positive on both ^{131}I WBS and PET/CT image. During follow-up, it was identified that three LNs progressed into PD following radiotherapy, while the uptake of ^{131}I WBS decreased (Fig. 3) and four nodes in the SD group demonstrated no significant changes in 18F-FDG PET/CT and a decreased uptake on the ^{131}I-WBS (Fig. 4).

Table III. Multivariate analysis of prognostic factors for patients with papillary thyroid cancer.

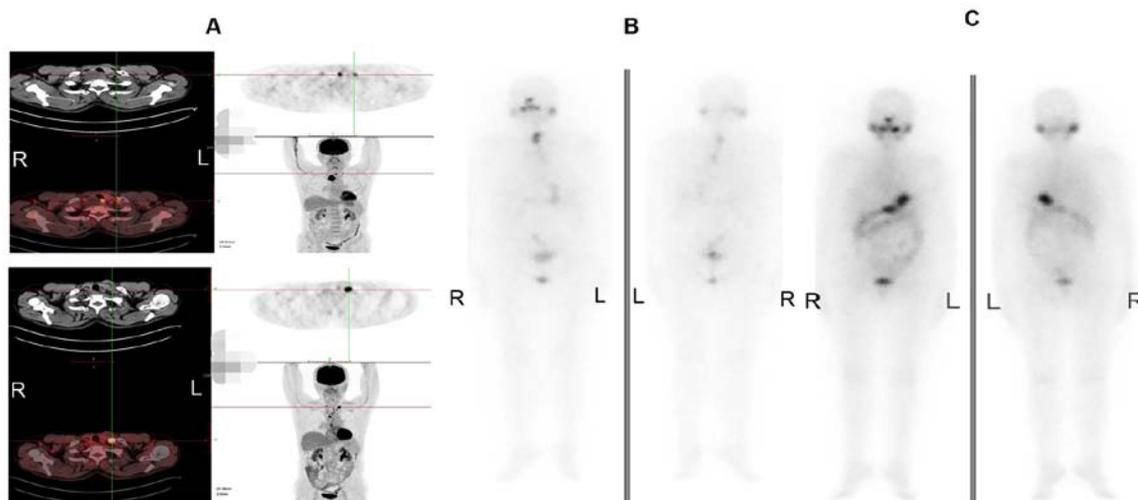| Characteristics	Odds ratio (95% confidence interval)	P-value
Standardized uptake value	1.194 (1.061-1.345)	0.003
Extrathyroidal extension	0.436 (0.206-0.923)	0.030
Age	-	0.268
Thyroglobulin	-	0.635
Sex	-	0.785
Spherical shape with solid density	-	0.874
Minimal axial diameter	-	0.300
Maximum axial diameter	-	0.510
In the central area	-	0.105
Punctate calcification	-	0.609
Longitudinal and transverse ratios (<2)	-	0.677
Residual thyroid tissue	-	0.274

Figure 3. A 58-year-old female patient with papillary thyroid carcinoma with a mLN. (A) LN was detected on the left side of the neck by CT with irregular shape and high density. (B) The standardized uptake values of the lesion on the PET/CT image before (upper image) and after (lower image) [131]I therapy were 4.8 and 15.4, respectively. [131]I WBS image revealed intermediate ^{131}I accumulations. (C) Following 6 months, the patient received 150 mCi ^{131}I therapy and WBS imaging demonstrated no uptake in the cervix. The lesion was defined as progressive disease. mLN, metastatic lymph node; LN, lymph node; PET, positron emission tomography; CT, computed tomography; ^{131}I, iodine-131; WBS, whole-body scan.
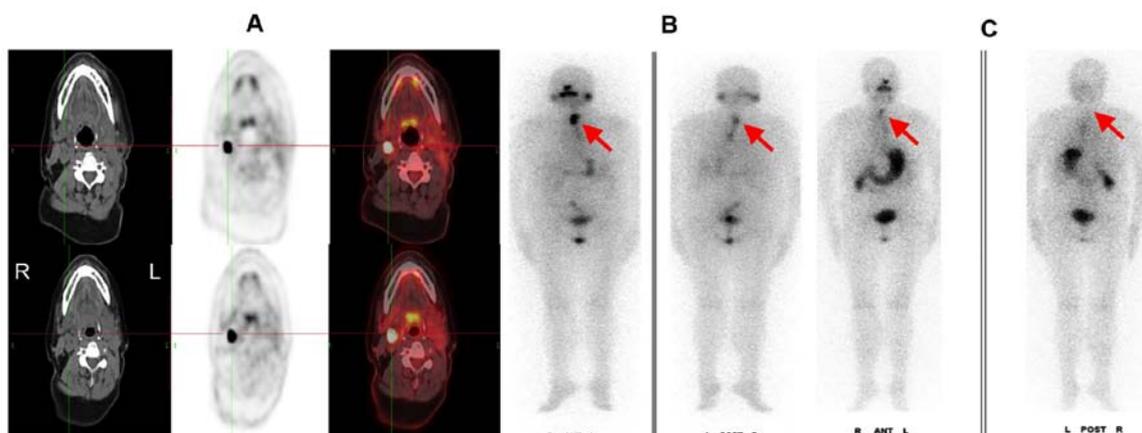
Figure 4. A 56-year-old female patient with papillary thyroid carcinoma with a mLN. CT revealed a LN with spherical shape and microcalcification in the right side of the neck. (A) The SULs of the LN (upper image) prior to and (lower image) following therapy were 47.2 and 47.6, respectively (the cross point). (B) First ^{131}I whole-body scan image revealed high ^{131}I accumulations in the cervix (red arrow). (C) Uptake of ^{131}I reduced following the second therapy, however the SUL was markedly higher (the red arrow). The lesion was defined as stable disease. SUL, standardized uptake value; mLN, metastatic lymph node; LN, lymph node; CT, computed tomography; ^{131}I, iodine-131.

Discussion

LN metastasis is common in patients with PTC (15). A previous study based on a Surveillance, Epidemiology, and End Results database with 14 years of follow-up demonstrated that an mLN can serve as a specific independent predictor for PTC, and the total survival rate of patients with mLNs was lower compared with patients without mLNs (hazard ratio, 12.597) (16). ^{18}F-FDG PET/CT is useful for detecting the sites of metastatic disease and recurrence, which appear on radio-iodine images (17). In the present study, all ^{18}F-FDG PET/CT acquisitions were performed under a TSH stimulated state and FDG uptake was positive in all patients with PTC with mLNs, while ^{131}I accumulation was identified in eight lesions from 6 patients on the first WBS. In addition, 42 mLNs demonstrated a minimum diameter ≤1 cm and 15 patients with a total of 27 LNs exhibited residual thyroid tissue and exhibited star emission in the thyroid bed area on ^{131}I WBS, which may explain why the majority of the LNs did not demonstrate positive ^{131}I on the initial WBS. Therefore, the present study attempted to use PET/CT imaging to predict the therapeutic effect of mLNs receiving ^{131}I radiotherapy.

At present, the most widely used imaging technologies for diagnosis of thyroid cacinoma with mLNs include ultrasonography, magnetic resonance imaging (MRI), CT, SPECT and PET/CT (18-22). Pathology is the gold standard for diagnosing LN metastasis of thyroid carcinoma (23). However, certain mLNs are located deep in the neck, which presents difficulties for diagnosis. Imaging examination serves an important role in the diagnosis and therapeutic evaluation of thyroid cancer LN metastasis. Mulla and Schulte (24) reported that ultrasonography in the diagnosis of cervical LN metastases exhibits a sensitivity of 63% and specificity of 93%. However, ultrasonography possesses limitations for the diagnosis of central compartment lymph nodal metastases, as certain LNs are located in deep regions, the trachea and surrounding structures (25). [131]I SPECT/CT has been used to evaluate patients with differentiated thyroid cancer (DTC); however, residual thyroid tissue following thyroidectomy affects the uptake of ^{131}I and imaging of mLNs (26). Compared with CT, which provides low-resolution images for soft tissue, MRI exhibits distinct advantages for the diagnosis of metastatic thyroid carcinoma, including high-resolution determination of soft tissue, no radiation exposure and a multi-sequence, multi-parameter imaging capability (27). For detection of cervical nodal metastasis in patients with DTC, MRI demonstrates a high sensitivity, accuracy, specificity and positive predictive value (19); however, MRI exhibits a low specificity and negative predictive value for the detection of lateral neck lymph nodal metastasis (28). PET/CT is useful in localizing metastasis that does not accumulate iodine in patients with elevated Tg levels (29) and has been demonstrated to have a specificity ≤90% (30). In the present study, mLNs were diagnosed by pathology, ultrasonography, CT, SPECT, PET/CT and clinical follow up. However, MRI was not analyzed in this study due to the limited number of patients examined.

The present study identified that the SULpeak of group A was significantly lower compared with that of group B prior to therapy. FDG is highly concentrated in cells with high glycolytic rates, including poorly differentiated,

proliferating thyroid cancer cells (31). The combination of a low iodine concentration and a high FDG concentration has been considered to be an indicator of poorly differentiated or dedifferentiated thyroid cancer cells (32), which typically indicates a poor prognosis. Therefore, a low uptake of ^{18}F-FDG in LNs indicates low tumor activity and a good prognosis for patients with PTC with mLNs. Sun *et al* (33) demonstrated that tumor/normal tissue (T/NT) of cervical LN metastases in ^{18}F-FDG dual-head coincidence imaging is associated with the efficacy of radioiodine therapy; a high T/NT indicates a poor therapeutic effect. Based on the present results, the cut-off value of mLNs, involved in SUL with or without ^{131}I accumulation, was >5.85 on the PET/CT image, which demonstrated improved sensitivity and specificity for predicting a poor prognosis following ^{131}I ablation.

The present results also demonstrated that a high SULpeak of mLNs and extrathyroidal extension following thyroid surgery were significant poor prognostic factors for patients receiving therapy. A number of previous studies have demonstrated that the ^{131}I WBS is negative for dedifferentiated PTC lesions that lack the ability to take up iodine and these dedifferentiated PTC lesions are ^{18}F-FDG-avid (32,34,35). The present study identified that certain mLNs demonstrated positive results in both imaging examinations; however, the therapeutic effect of these mLNs has rarely been reported. In the present study, among the eight positive mLNs revealed by ^{131}I-WBS, two maintained SD, one achieved CR and the other five progressed to PD. A possible reason for this poor prognosis may be that the LN metastases had a lack of oxygen or were poorly differentiated, which reduced the effectiveness of ^{131}I and led to a poorer curative effect. Of the 42 negative ^{131}I WBS, ten LNs achieved CR, 11 reached a PR, 16 remained in SD and five developed into PD. Only eight LNs possessed a minimum diameter ≥10 mm and 27 LNs displayed a star emission image in the thyroid bed area on the ^{131}I WBS, which may have led to the majority of the LNs not being ^{131}I-positive on the initial WBS. During subsequent therapy, ^{131}I accumulation was observed in two mLNs, which were negative on the first ^{131}I WBS and had SULpeaks, of 5.5 and 5.3, respectively on the PET/CT prior to therapy. Finally, both LNs achieved CR (Fig. 2).

A number of previous studies have confirmed that macroscopic LN metastasis is a predictor that is specifically associated with PTC persistence or recurrence (36-40). Wu *et al* (41) investigated prognostic factors of ^{131}I treatment for cervical LN metastases of PTC and suggested that the therapeutic effectiveness was associated with the size of the mLNs. However, the present results revealed that patients with a high SULpeak and a history of extrathyroidal extension exhibited a poorer therapeutic effect following ^{131}I ablation. mLNs with a SULpeak >5.85 could be considered as poor prognostic factors for therapy with or without a positive ^{131}I result. Furthermore, seven mLNs from 4 patients with PTC were both positive on ^{131}I WBS and PET/CT, which demonstrated no remission following ^{131}I therapy. These lesions may be associated with more aggressive characteristics and ^{131}I therapy appears to have little to no effect on the viability of such lesions (42).

The present study had a number of limitations. Firstly, the number of subjects was small as only 50 mLNs were involved

from 32 patients with PTC, which may lead to missing ^{131}I on SPECT imaging due to a low resolution. In addition, the pathological characteristics of the primary tumor and LNs were not completely analyzed due to the limited number of samples. Furthermore, the present study was retrospective in nature and excluded certain imaging methods that could additionally be performed, including ultrasound, CT and MRI. Therefore, future studies should aim to compare the predictive value of various imaging examinations for the prognosis of thyroid carcinoma with LN metastases.

In conclusion, a high SULpeak and spherical shape with a solid density of mLNs were identified as risk predictors for the clinical outcome of patients with PTC treated with radioiodine therapy, regardless of whether ^{131}I dose has accumulated on those nodes. When the SULpeak was >5.85, a poor therapeutic effect was revealed for mLNs. Therefore, patients with a high SULpeak of LNs and extrathyroidal extension may be considered to exhibit a poor prognosis. By introducing associated factors of mLNs on the predictive value of PET/CET, these may exhibit a useful role in the management of PTC. Further studies should focus on the detection of LNs with two positive images to identify the association between mLNs and the clinical outcome following ^{131}I therapy.

Availability of data and materials

The datasets used and analyzed during the present study are available from the corresponding author on reasonable request.

Authors' contributions

CL contributed to the study design and wrote the manuscript. JZ collected and analyzed the clinical data of patients. HW was responsible for the statistical analysis of the data and revising for important intellectual content. All authors read and approved the final manuscript.

Ethics approval and consent to participate

The approvals of all patients were waived due to the retrospective nature of this study. The research protocol was approved by Ethics Committee of Xinhua Hospital Affiliated to Shanghai Jiaotong University School of Medicine (Shaghai, China).

Patient consent for publication

Not applicable.

Competing interests

The authors declare that they have no competing interests.

References

1. Kitahara CM and Sosa JA: The changing incidence of thyroid cancer. Nat Rev Endocrinol 12: 646-653, 2016.
2. Schneider DF, Chen H and Sippel RS: Impact of lymph node ratio on survival in papillary thyroid cancer. Ann Surg Oncol 20: 1906-1911, 2013.
3. Lee YM, Lo CY, Lam KY, Wan KY and Tam PK: Well-differentiated thyroid carcinoma in Hong Kong Chinese patients under 21 years of age: A 35-year experience. J Am Coll Surg 194: 711-716, 2002.
4. Mazzaferri EL and Massoll N: Management of papillary and follicular (differentiated) thyroid cancer: New paradigms using recombinant human thyrotropin. Endocr Relat Cancer 9: 227-247, 2002.
5. Giannoula E, Iakovou I and Verburg FA: Long term quality of life in differentiated thyroid cancer patients after thyroidectomy and high doses of ^{131}I with or without suppressive treatment. Hell J Nucl Med 21: 69-73, 2018.
6. Ronga G, Toteda M, D'Apollo R, De Cristofaro F, Filesi M, Acqualagna G, Argirò R, Ciancamerla M, Ugolini F, Montesano T: Lymph node metastases from differentiated thyroid carcinoma: Does radioiodine still play a role? Clin Ter 163: 377-381, 2012.
7. Kim WG, Ryu JS, Kim EY, Lee JH, Baek JH, Yoon JH, Hong SJ, Kim ES, Kim TY, Kim WB and Shong YK: Empiric high-dose 131-iodine therapy lacks efficacy for treated papillary thyroid cancer patients with detectable serum thyroglobulin, but negative cervical sonography and 18F-fluorodeoxyglucose positron emission tomography scan. J Clin Endocrinol Metab 95: 1169-1173, 2010.
8. Bertagna F, Albano D, Bosio G, Piccardo A, Dib B and Giubbini R: 18F-FDG-PET/CT in patients affected by differentiated thyroid carcinoma with positive thyroglobulin level and negative 131I whole body scan. It's value confirmed by a bicentric experience. Curr Radiopharm 9: 228-234, 2016.
9. Xu YH, Shen CT, Xue YL, Qiu ZL and Luo QY: Iodine-131 SPET/CT and 18F-FDG PET/CT for the identification and localization of mediastinal lymph node metastases from differentiated thyroid carcinoma. Hell J Nucl Med 16: 199-203, 2013.
10. Wang QC, Cheng W, Wen X, Li JB, Jing H and Nie CL: Shorter distance between the nodule and capsule has greater risk of cervical lymph node metastasis in papillary thyroid carcinoma. Asian Pac J Cancer Prev 15: 855-860, 2014.
11. van den Brekel MW, Stel HV, Castelijns JA, Nauta JJ, van der Waal I, Valk J, Meyer CJ and Snow GB: Cervical lymph node metastasis: Assessment of radiologic criteria. Radiology 177: 379-384, 1990.
12. Lodge MA, Chaudhry MA and Wahl RL: Noise considerations for PET quantification using maximum and peak standardized uptake value. J Nucl Med 53: 1041-1047, 2012.
13. Turk A, Asa SL, Baloch ZW, Faquin WC, Fellegara G, Ghossein RA, Giordano TJ, LiVolsi VA, Lloyd R, Mete O, et al: Interobserver variability in the histopathologic assessment of extrathyroidal extension of well differentiated thyroid carcinoma supports the new american joint committee on cancer eighth edition criteria for tumor staging. Thyroid, Apr 27, 2019 (Epub ahead of print).
14. Wahl RL, Jacene H, Kasamon Y and Lodge MA: From RECIST to PERCIST: Evolving considerations for PET response criteria in solid tumors. J Nucl Med 50 (Suppl 1): 122S-150S, 2009.
15. Shaha AR: Prognostic factors in papillary thyroid carcinoma and implications of large nodal metastasis. Surgery 135: 237-239, 2004.
16. Podnos YD, Smith D, Wagman LD and Ellenhorn JD: The implication of lymph node metastasis on survival in patients with well-differentiated thyroid cancer. Am Surg 71: 731-734, 2005.
17. Shammas A, Degirmenci B, Mountz JM, McCook BM, Branstetter B, Bencherif B, Joyce JM, Carty SE, Kuffner HA and Avril N: 18F-FDG PET/CT in patients with suspected recurrent or metastatic well-differentiated thyroid cancer. J Nucl Med 48: 221-226, 2007.
18. Zhao H and Li H: Meta-analysis of ultrasound for cervical lymph nodes in papillary thyroid cancer: Diagnosis of central and lateral compartment nodal metastases. Eur J Radiol 112: 14-21, 2019.
19. Renkonen S, Lindén R, Bäck L, Silén R, Mäenpää H, Tapiovaara L and Aro K: Accuracy of preoperative MRI to assess lateral neck metastases in papillary thyroid carcinoma. Eur Arch Otorhinolaryngol 274: 3977-3983, 2017.

20. Hempel JM, Kloeckner R, Krick S, Pinto Dos Santos D, Schadmand-Fischer S, Boeßert P, Bisdas S, Weber MM, Fottner C, Musholt TJ, *et al*: Impact of combined FDG-PET/CT and MRI on the detection of local recurrence and nodal metastases in thyroid cancer. Cancer Imaging 16: 37, 2016.
21. Lou K, Gu Y, Hu Y, Wang S and Shi H: Technetium-99m-pertechnetate whole-body SPET/CT scan in thyroidectomized differentiated thyroid cancer patients is a useful imaging modality in detecting remnant thyroid tissue, nodal and distant metastases before ^{131}I therapy. A study of 416 patients. Hell J Nucl Med 21: 121-124, 2018.
22. Lee Y, Kim JH, Baek JH, Jung SL, Park SW, Kim J, Yun TJ, Ha EJ, Lee KE, Kwon SY, *et al*: Value of CT added to ultrasonography for the diagnosis of lymph node metastasis in patients with thyroid cancer. Head Neck 40: 2137-2148, 2018.
23. Garau LM, Rubello D, Morganti R, Boni G, Volterrani D, Colletti PM and Manca G: Sentinel lymph node biopsy in small papillary thyroid cancer: A meta-analysis. Clin Nucl Med 44: 107-118, 2019.
24. Mulla M and Schulte KM: The accuracy of ultrasonography in the preoperative diagnosis of cervical lymph node (LN) metastasis in patients with papillary thyroid carcinoma: A meta-analysis. Eur J Radiol 81: 1965; author reply 1966, 2012.
25. Na DK, Choi YJ, Choi SH, Kook SH and Park HJ: Evaluation of cervical lymph node metastasis in thyroid cancer patients using real-time CT-navigated ultrasonography: Preliminary study. Ultrasonography 34: 39-44, 2015.
26. He Y, Pan MZ, Huang JM, Xie P, Zhang F and Wei LG: Iodine-131: An effective method for treating lymph node metastases of differentiated thyroid cancer. Med Sci Monit 22: 4924-4928, 2016.
27. Hoang JK, Vanka J, Ludwig BJ and Glastonbury CM: Evaluation of cervical lymph nodes in head and neck cancer with CT and MRI: Tips, traps, and a systematic approach. AJR Am J Roentgenol 200: W17-W25, 2013.
28. Mihailovic J, Prvulovic M, Ivkovic M, Markoski B and Martinov D: MRI versus ^{131}I whole-body scintigraphy for the detection of lymph node recurrences in differentiated thyroid carcinoma. AJR Am J Roentgenol 195: 1197-1203, 2010.
29. Freudenberg LS, Antoch G, Frilling A, Jentzen W, Rosenbaum SJ, Kühl H, Bockisch A and Görges R: Combined metabolic and morphologic imaging in thyroid carcinoma patients with elevated serum thyroglobulin and negative cervical ultrasonography: Role of 124I-PET/CT and FDG-PET. Eur J Nucl Med Mol Imaging 35: 950-957, 2008.
30. Morita S, Mizoguchi K, Suzuki M and Iizuka K: The accuracy of (18)[F]-fluoro-2-deoxy-D-glucose-positron emission tomography/computed tomography, ultrasonography and enhanced computed tomography alone in the preoperative diagnosis of cervical lymph node metastasis in patients with papillary thyroid carcinoma. World J Surg 34: 2564-2569, 2010.
31. Wang W, Larson SM, Tuttle RM, Kalaigian H, Kolbert K, Sonenberg M and Robbins RJ Resistance of [18f]-fluorodeoxy-glucose-avid metastatic thyroid cancer lesions to treatment with high-dose radioactive iodine. Thyroid 11: 1169-1175, 2001.

32. Feine U, Lietzenmayer R, Hanke JP, Held J, Wöhrle H and Müller-Schauenburg W: Fluorine-18-FDG and iodine-131-iodide uptake in thyroid cancer. J Nucl Med 37: 1468-1472, 1996.
33. Sun YG, Feng HJ, Liu JH, Hu R and Ouyang W: Value of (18) F-FDG dual head coincidence imaging in predicting the efficacy of radioiodine therapy for papillary thyroid carcinoma with cervical lymph node metastasis. Nan Fang Yi Ke Da Xue Xue Bao 31: 1571-1574, 2011 (In Chinese).
34. Weigel RJ and McDougall IR: The role of radioactive iodine in the treatment of well-differentiated thyroid cancer. Surg Oncol Clin N Am 15: 625-638, 2006.
35. Wang W, Macapinlac H, Larson SM, Yeh SD, Akhurst T, Finn RD, Rosai J and Robbins RJ: [18F]-2-fluoro-2-deoxy-D-glucose positron emission tomography localizes residual thyroid cancer in patients with negative diagnostic (131)I whole body scans and elevated serum thyroglobulin levels. J Clin Endocrinol Metab 84: 2291-2302, 1999.
36. Mazzaferri EL and Jhiang SM: Long-term impact of initial surgical and medical therapy on papillary and follicular thyroid cancer. Am J Med 97: 418-428, 1994.
37. Bardet S, Ciappuccini R, Quak E, Rame JP, Blanchard D, de Raucourt D, Babin E, Michels JJ, Vaur D and Heutte N: Prognostic value of microscopic lymph node involvement in patients with papillary thyroid cancer. J Clin Endocrinol Metab 100: 132-140, 2015.
38. Ito Y, Miyauchi A, Jikuzono T, Higashiyama T, Takamura Y, Miya A, Kobayashi K, Matsuzuka F, Ichihara K and Kuma K: Risk factors contributing to a poor prognosis of papillary thyroid carcinoma: Validity of UICC/AJCC TNM classification and stage grouping. World J Surg 31: 838-848, 2007.
39. de Meer SG, Dauwan M, de Keizer B, Valk GD, Borel Rinkes IH and Vriens MR: Not the number but the location of lymph nodes matters for recurrence rate and disease-free survival in patients with differentiated thyroid cancer. World J Surg 36: 1262-1267, 2012.
40. de Castro TP, Waissmann W, Simões TC, de Mello RC and Carvalho DP: Predictors for papillary thyroid cancer persistence and recurrence: A retrospective analysis with a 10-year follow-up cohort study. Clin Endocrinol (Oxf) 85: 466-474, 2016.
41. Wu Q, Zhang YM, Sun S, Li JJ, Wu J, Li X, Zhu S, Wei W and Sun SR: Clinical and sonographic assessment of cervical lymph node metastasis in papillary thyroid carcinoma. J Huazhong Univ Sci Technolog Med Sci 36: 823-827, 2016.
42. Diab Y: Sentinel lymph nodes mapping in cervical cancer a comprehensive review. Int J Gynecol Cancer 27: 154-158, 2017.